

# Novel Insights into the Basis for *Escherichia coli* Superoxide Dismutase's Metal Ion Specificity from Mn-Substituted FeSOD and Its Very High $E_m$ <sup>†</sup>

Carrie K. Vance<sup>‡,§</sup> and Anne-Frances Miller<sup>\*,‡,||</sup>

Departments of Chemistry and Biophysics, The Johns Hopkins University, 3400 North Charles Street, Baltimore, Maryland 21218, and Department of Chemistry, University of Kentucky, Lexington, Kentucky 40506-0055

Received June 25, 2001; Revised Manuscript Received August 13, 2001

**ABSTRACT:** Fe and Mn are both entrained to the same chemical reaction in apparently superimposable superoxide dismutase (SOD) proteins. However, neither Fe-substituted MnSOD nor Mn-substituted FeSOD is active. We have proposed that the two SOD proteins must apply very different redox tuning to their respective metal ions and that tuning appropriate for one metal ion results in a reduction potential ( $E_m$ ) for the other metal ion that is either too low (Fe) or too high (Mn) [Vance and Miller (1998) *J. Am. Chem. Soc.* 120, 461–467]. We have demonstrated that this is true for Fe-substituted MnSOD from *Escherichia coli* and that this metal ion–protein combination retains the ability to reduce but not oxidize superoxide. We now demonstrate that the corollary is also true: Mn-substituted FeSOD [Mn(Fe)SOD] has a very high  $E_m$ . Specifically, we have measured the  $E_m$  of *E. coli* MnSOD to be 290 mV vs NHE. We have generated Mn(Fe)SOD and find that Mn is bound in an environment similar to that of the native (Mn)SOD protein. However, the  $E_m$  is greater than 960 mV vs NHE and much higher than MnSOD's  $E_m$  of 290 mV. We propose that the different tuning stems from different hydrogen bonding between the proteins and a molecule of solvent that is coordinated to the metal ion in both cases. Because a proton is taken up by SOD upon reduction, the protein can exert very strong control over the  $E_m$ , by modulating the degree to which coordinated solvent is protonated, in both oxidation states. Thus, coordinated solvent molecules may have widespread significance as “adapters” by which proteins can control the reactivity of bound metal ions.

Life is opportunistic, and there are many examples of the same reaction being catalyzed by different redox-active cofactors. In many cases the analogous enzymes or electron-carrier proteins are unrelated: Fe and Mn catalase (2–4), flavin- or Fe-based hydroxylases (5–7), and hydrogenases employing Ni and Fe vs Fe only [which serve to mediate the same reaction but in opposite directions (8, 9)]. This is natural as different protein environments are required to accommodate different cofactors and complement their individual chemical characteristics. However, there are a number of cases in which enzymes that employ different metal ions for the same reaction are highly homologous: Mo-containing nitrogenase, V-containing nitrogenase, and the Fe-nitrogenase (10).

Consistent with the tendency of Fe to be a limiting nutrient, especially in oxidizing environments (11, 12), many high-potential Fe-containing enzymes have non-Fe-containing analogues. Several of the Mn-containing analogues are also

homologues (13, 14). However, in general, redox-active Mn seems to function as an oxidant in enzymes, and Mn does not occur biologically at potentials as low as those of the low-potential Fe enzymes.<sup>1</sup>

Superoxide dismutase (SOD)<sup>2</sup> is the best understood case in which Fe and Mn occur in homologous proteins and engage in the same chemistry using the same oxidation states. This may reflect the fact that superoxide dismutation includes two half-reactions, one oxidative and the other reductive, each of which would be spontaneous for one metal ion and

<sup>1</sup> By nature,  $d^5$   $Mn^{2+}$  is less reducing than  $d^6$   $Fe^{2+}$ , and  $d^6$   $Mn^{1+}$  is biologically inaccessible. However, there are too few well-characterized Mn enzymes to support a detailed comparison of the biochemical possibilities of Fe and Mn. Moreover, even this limited set may be seriously biased since some Mn enzymes appear to be derived from Fe enzymes (or vice versa). In addition, Fe tends to be more abundant than Mn in reducing environments, so organisms with low-potential metabolisms would experience much less pressure to develop Mn enzymes.

<sup>2</sup> Abbreviations: CAPS, 3-(cyclohexylamino)-1-propanesulfonic acid; DCIP, 2,6-dichloroindophenol; DPPH,  $\alpha,\alpha'$ -diphenyl- $\beta$ -picrylhydrazine; EDTA, ethylenediaminetetraacetic acid;  $E_m$ , reduction potential; EPR, electron paramagnetic resonance spectroscopy; FeSOD, native Fe-containing superoxide dismutase; (Fe)SOD, the protein of FeSOD; Fe(Mn)SOD, Fe-substituted (Mn)SOD protein; MCD, magnetic circular dichroism; MnSOD, native Mn-containing SOD; (Mn)SOD, the protein of MnSOD; Mn(Fe)SOD, Mn-substituted (Fe)SOD protein; MV, methyl viologen; NHE, normal hydrogen electrode; pBQ, *p*-benzoquinone; TMPD,  $N,N',N',N'$ -tetramethylphenylenediamine; Tris, tris-(hydroxymethyl)aminomethane.

<sup>†</sup> Acknowledgment is made to the donors of the Petroleum Research Fund, administered by the American Chemical Society, for partial support of this research under ACS-PRF 33266-AC4.3. A.-F.M. is pleased to thank the NSF for financial support (MCB9728793).

\* To whom correspondence should be addressed at the Department of Chemistry, University of Kentucky, Lexington, KY 40506-0055. E-mail: afm@pop.uky.edu. Fax: (859) 323-1069. Tel: (859) 257-9349.

<sup>‡</sup> The Johns Hopkins University.

<sup>§</sup> Current address: Center for Research of Endangered Wildlife, Cincinnati Zoo and Botanical Garden, Cincinnati, OH.

<sup>||</sup> University of Kentucky.

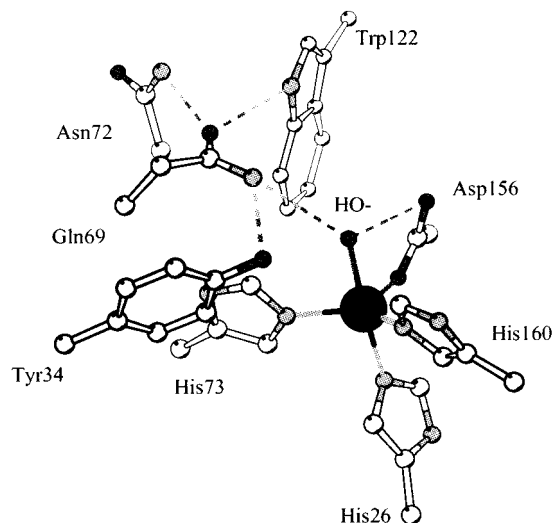
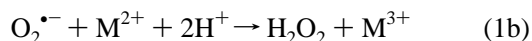
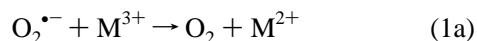


FIGURE 1: Cartoon of the FeSOD active site based on the coordinates in ref 17 and showing the hydrogen-bonding network supporting the coordinated solvent. The large dark ball is Fe, the dark gray balls are N, and the light gray balls are O. Hydrogens are not shown for clarity. Residue numbers are those of FeSOD.

the other of which may be imposed (at some cost to the first) by the protein.<sup>3</sup>

SOD catalyzes the disproportionation of  $2\text{O}_2^{\bullet-} + 2\text{H}^+ \rightarrow \text{O}_2 + \text{H}_2\text{O}_2$  in a two-step reaction in which the metal ion ( $\text{M} = \text{Fe}$  or  $\text{Mn}$  here) cycles between the 2+ and 3+ oxidation states (15).



Thus, the  $E_m$ <sup>4</sup> of Fe or Mn must lie between those of  $\text{O}_2/\text{O}_2^{\bullet-}$  and  $(\text{O}_2^{\bullet-} + 2\text{H}^+)/\text{H}_2\text{O}_2$  in order for the enzyme to function (16). Fe (or Mn) is coordinated in a trigonal bipyramid by three histidines, an Asp<sup>-</sup>, and a molecule of solvent. The solvent is believed to be  $\text{OH}^-$  in the oxidized enzyme and to become  $\text{H}_2\text{O}$  upon reduction (17). The active sites of FeSOD and MnSOD display the same geometry with respect not only to the ligands but also to the general locations of second-sphere functionalities including a conserved Tyr and a Gln which hydrogen bonds to the coordinated solvent (Figure 1). The overall protein structures of FeSOD and MnSOD are also homologous (18).

FeSODs and MnSODs have each been prepared with the other metal ion bound. Fe-substituted MnSOD [Fe(Mn)SOD] from *Escherichia coli* was first reported by Ose and Fridovich (19), and Mn-substituted *Pseudomonas ovalis* FeSOD [Mn(Fe)SOD] was first prepared by Yamakura (20), but both were found to be inactive. By contrast, the SODs from a number of anaerobes display activity with either Fe or Mn and are therefore called “cambialistic” (21–25). Mutants of *E. coli* MnSOD have been produced that have significant

low activity with the non-native metal ion, in the standard assay (26–28), and a mutant of the cambialistic SOD from *Porphyromonas gingivalis* was shown to have greater activity with Mn (27). These comparisons of mutant and native proteins with Fe bound seek to identify the roles of specific amino acids in determining the reactivity of the metal ion. They have led to proposals that Fe is inactive in (Mn)SOD protein due to depression of the pK governing  $\text{OH}^-$  binding (29), non-native ligand basicity due to Tyr34 (28), or a non-native coordination geometry (1, 30).

We have proposed that non-native protein–metal ion combinations are inactive because application of the redox tuning appropriate to the native metal ion results in non-native metal ion having an  $E_m$  that is much too high or low to mediate both half-reactions 1a and 1b (31). Indeed, we found that *E. coli* Fe(Mn)SOD has an  $E_m$  of  $-220$  mV, almost half a volt lower than FeSOD’s and lower than the  $E_m$  required for oxidation of  $\text{O}_2^{\bullet-}$  to  $\text{O}_2$ . As predicted, Fe(Mn)SOD retains the ability to reduce  $\text{O}_2^{\bullet-}$ . Thus, Fe(Mn)SOD’s inability to disproportionate  $\text{O}_2^{\bullet-}$  can be explained by its specific inability to oxidize it (31). The current findings complete the proof of the model and permit its generalization to Mn by showing that Mn(Fe)SOD’s  $E_m$  is much higher than that of *E. coli* MnSOD.

SOD represents an exceptionally small and simple example of the widespread phenomenon of utilizing alternate metal ions to do the same job. With both Fe(Mn)SOD and Mn(Fe)SOD in hand, as well as FeSOD and MnSOD, we are now able to examine chemical strategies used to support SOD activity from two independent perspectives, that of metal ion substitution and that of protein replacement. The very different redox tuning applied by two highly homologous proteins makes *E. coli*’s SODs an exceptionally useful system, in which the  $E_m$  may be correlated with a limited number of amino acid differences which occur without major structural reorganization. Thus, these studies pave the way to using metal ion substitution and intentional redox tuning by mutagenesis to modify existing enzymes to catalyze novel, desired chemistry.

## MATERIALS AND METHODS

*Preparation of Mn-Substituted (Fe)SOD.* Mn- and FeSOD were purified as described previously (31–34) and typically had activities of 6000 and 7000 units/(mg of protein·min), respectively, in the standard assay (35). Fe(Mn)SOD was prepared as before (30, 31). Fe was removed from FeSOD and replaced by Mn using variations of the alkaline denaturing protocol of Yamakura (20). A 5 mL aliquot of 0.2 mM FeSOD was diluted with 20 mL of degassed 250 mM pH 11.2 carbonate buffer containing 10 mM EDTA or DPTA in a 30 mL Wheaton vial. Sodium dithionite was added to 1 mM, and the solution was heated in a water bath for 1.5 h at 37 °C.  $\text{MnCl}_2$  was added to a final concentration of 2 mM, and the solution was allowed to sit on the bench for 10 min before being dialyzed against 50 mM pH 9.4 Tris-HCl buffer and then against Millipore-purified distilled water.  $\text{Mn}(\text{OH})_2$  precipitate was centrifuged out, and the solution of Mn(Fe)SOD was filtered before dialysis into the final working buffer of 100 mM potassium phosphate at pH 7.8.

*EPR Spectra of (Reduced)  $\text{Mn}^{2+}$  in (Fe)SOD and (Mn)-SOD.* EPR spectra were collected on a Bruker 300MX

<sup>3</sup> All redox enzymes must of course be regenerated by a restorative redox reaction, but the latter may be driven by use of a strong reductive or oxidative agent, unlike SOD’s case in which the oxidant and the reductant are both  $\text{O}_2^{\bullet-}$ .

<sup>4</sup> The  $E_m$ , or reduction potential, signifies the electron acceptor strength of a compound. Thus it is analogous to the pK, except that it applies to electron acquisition instead of  $\text{H}^+$  acquisition.

calibrated at  $g = 2.00$  using DPPH and at  $g = 6$  using myoglobin in 100 mM phosphate buffer. Samples of  $\approx 200 \mu\text{M}$   $\text{Mn}^{2+}$ SOD dimers in 100 mM potassium phosphate buffer at pH 7.8 were reduced by dithionite or  $\text{H}_2\text{O}_2$ .  $\text{Mn}^{2+}$ -(Fe)SOD samples were prepared similarly but did not require reduction. The pH of each sample was measured before freezing and again after EPR spectroscopy and thawing with a pH microelectrode. EPR spectra were collected at 65 K in an Air-Products liquid He cryostat cooled with liquid  $\text{N}_2$ . Each spectrum was collected at 9.48 GHz using 40 mW nominal power and 10 G modulation at 100 kHz, with the center field at 5000 G and a sweep width of 10 000 G. Baseline corrections for  $\text{Mn}^{2+}$ SOD were made on the basis of a high-quality reference spectrum of 4 mM  $\text{Mn}^{2+}$ SOD prepared as above but observed at 4 K. The appearance of this spectrum was the same as that of spectra collected at 65 K but with much better signal-to-noise ratio. Baseline correction is difficult to do well for the broad rolling signals above 4000 G; therefore, this region was not used for quantitative analyses.

*Optical Spectra of (Oxidized)  $\text{Mn}^{3+}$  in (Fe)SOD and (Mn)-SOD.* Visible absorption spectra were collected on a Hewlett-Packard 8452A diode array spectrophotometer equipped with a thermostated cell compartment equilibrated at 25 °C. The optical spectrum of  $\text{Mn}^{3+}$ (Fe)SOD was taken after the sample had been deaerated, oxidized by titration with a fresh solution of  $\text{KMnO}_4$ , and sealed under argon. The pH was measured using a combination pH microelectrode fitted into a 12 gauge stainless steel needle (Microelectrodes Inc.).  $\text{Mn}^{3+}$ SOD and  $\text{Mn}^{3+}$ (Fe)SOD were buffered with 100 mM pH 7.8 potassium phosphate in Millipore-purified  $\text{H}_2\text{O}$ . Protein concentrations ranged from 100 to 500  $\mu\text{M}$  in dimers based on an  $\epsilon_{280} = 86\,600 \text{ M}^{-1} \text{ cm}^{-1}$  for MnSOD (34, 36) and  $\epsilon_{280} = 101\,000 \text{ M}^{-1} \text{ cm}^{-1}$  for FeSOD and Mn(Fe)SOD (33).

*Reduction Potential Measurements.* Possible mediators were first characterized with respect to their  $E_m$ , extinction coefficients, solubility, and stability in 100 mM phosphate buffer at pH 7.8 with 100 mM KCl. Cyclic voltammetry (CV) was used to measure the  $E_m$  of the mediator and ascertain the reversibility of its redox couple under these conditions. Candidate mediators' abilities to equilibrate with MnSOD were tested in the experimental apparatus used previously for FeSOD (3, 4, 31). Typically, 3 mL of 200  $\mu\text{M}$  MnSOD in 100 mM phosphate buffer at pH 7.8 with 100 mM KCl was deoxygenated and either reduced with methyl viologen semiquinone ( $\text{MV}^\bullet$ ) or used "as is" in its native mixture of  $\approx 80\%$  oxidized and 20% reduced states. Substoichiometric amounts of deoxygenated mediator from freshly prepared stock solutions were then added, and optical and/or EPR spectra of the mixture were observed as a function of time, to assess the approach to equilibrium and the chemical stability of the mediator. The electrochemical potential was recorded continuously, and the concentration of oxidized MnSOD was determined by deconvolution of the optical spectrum into the signals of  $\text{Mn}^{3+}$ SOD and the mediator and then application of  $\text{Mn}^{3+}$ SOD's extinction coefficient of  $850 \text{ M}^{-1} \text{ cm}^{-1}$  at 478 nm ( $=\lambda_{\text{max}}$ ) (34). Alternately, the concentration of  $\text{Mn}^{2+}$ SOD was measured by EPR. The total concentration of MnSOD was determined in advance from the  $A_{280}$  and  $\epsilon_{280} = 86\,600 \text{ M}^{-1} \text{ cm}^{-1}$  (34). Parallel experiments were performed without MnSOD present to assess the mediator's

stability and to obtain their optical signals uncomplicated by that of  $\text{Mn}^{3+}$ SOD for use in the deconvolutions.

Redox titrations of MnSOD using pBQ as the mediator were conducted in the same anaerobic cuvette as described above. Deoxygenated pBQ was added to 2 mM final concentration to 6 mL of deoxygenated MnSOD at 630  $\mu\text{M}$  in dimers which had been preoxidized with  $\text{KMnO}_4$ . The titration was performed by repeated additions of 20  $\mu\text{L}$  aliquots of electrochemically generated 6 mM  $\text{MV}^\bullet$ , and the potential and optical spectrum were used to monitor the approach to equilibrium at each step. The system was judged to have equilibrated when the electrode drift stabilized at  $\pm 5 \text{ mV}$  per hour (this usually took  $\approx 5 \text{ h}$ ). In an experiment of this long duration (2–3 days total), chemical changes in the pBQ result in significant changes in its optical spectrum, which overlaps that of  $\text{Mn}^{3+}$ SOD. Therefore, the fractional reduction of MnSOD was evaluated by EPR. Samples (300  $\mu\text{L}$ ) of the titration mixture were transferred anaerobically to Ar-filled EPR tubes and frozen under Ar in liquid  $\text{N}_2$ . The fractional reduction of MnSOD was calculated on the basis of the amplitude of the strong  $\text{Mn}^{2+}$  features near 1500 G, far from the signal of  $\text{BQ}^\bullet$  near 3400 G, relative to that of a sample of the same MnSOD solution which had been fully reduced with dithionite instead of being oxidized.

The titration was continued until EPR spectroscopy indicated formation of 100%  $\text{Mn}^{2+}$ SOD at 167 mV vs NHE. MnSOD was then reoxidized in steps by adding 20  $\mu\text{L}$  aliquots of anaerobic 6 mM aqueous  $\text{KMnO}_4$  to a potential of 508 mV vs NHE. As in the reductive titration, the potential and optical spectrum were used to monitor the approach to equilibrium, while the percent  $\text{Mn}^{2+}$ SOD was quantified by EPR. Finally, more 6 mM  $\text{MV}^\bullet$  was added, and the MnSOD was reduced again for several steps ending at 295 mV. The  $E_m$  of MnSOD was calculated by fitting the percent reduced MnSOD vs potential data with the Nernst equation assuming a single electron transfer event, as described for the case of FeSOD (31).

Limits on the  $E_m$  of Mn(Fe)SOD were established by attempting to oxidize it with oxidizing agents covering a range of potentials. All were first tested to confirm that they were able to oxidize MnSOD and, thus, rule out steric or electrostatic barriers to interaction with the very similar Mn-(Fe)SOD.  $\text{Mo}(\text{CN})_8^{3-}$  was prepared by oxidizing  $\text{K}_4\text{Mo}(\text{CN})_8$  potentiometrically or chemically with permanganate (34), shortly before addition to  $\text{Mn}^{2+}$ SOD. Ability to oxidize  $\text{Mn}^{2+}$ SOD was evaluated optically by monitoring the absorbance at 478 nm where  $\text{Mn}^{3+}$ SOD absorbs maximally and the decrease in the signal intensity of the oxidized form of the oxidant being tested. Successful oxidants of  $\text{Mn}^{2+}$ SOD were then applied similarly to  $\text{Mn}^{2+}$ (Fe)SOD, and the absorption spectrum was examined for changes. New spectral features not due to the oxidants and their derivatives were ascribed to  $\text{Mn}^{3+}$ (Fe)SOD.

## RESULTS

*Characterization of Mn(Fe)SOD.* We have generated Mn-(Fe)SOD with no residual Fe. It is colorless as prepared, suggesting that the  $\approx 0.5$  Mn per site is present as  $\text{Mn}^{2+}$ , as also observed by Yamakura for *P. ovalis* Mn(Fe)SOD (37). The presence of  $\text{Mn}^{2+}$  is confirmed by the EPR data in Figure 2. The EPR spectrum of  $\text{Mn}^{2+}$ (Fe)SOD lacks the six-line

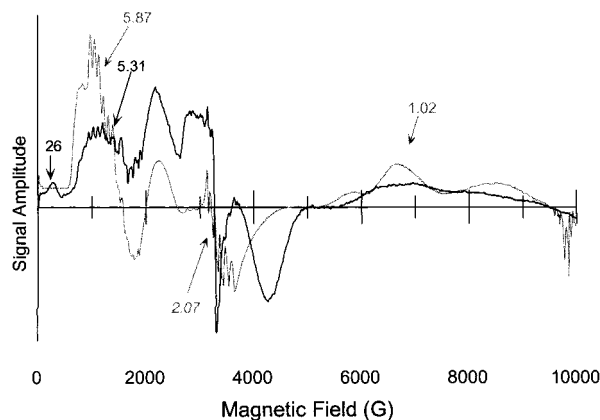


FIGURE 2: Comparison of the EPR spectra of  $\text{Mn}^{2+}$ (SOD) (thin gray line) and  $\text{Mn}^{2+}$ (Fe)SOD (heavy black line). 4 mM  $\text{Mn}^{2+}$ SOD in phosphate buffer at pH 7.8 was reduced with  $\text{H}_2\text{O}_2$  and rapidly frozen in liquid  $\text{N}_2$ . The spectrum was collected at 4 K using a nominal microwave power of 20 mW and 10 G modulation amplitude, as described in the Materials and Methods section.  $\text{Mn}^{2+}$ -(Fe)SOD at 0.4 mM in dimers was observed at 65 K as described in the Materials and Methods section. The two spectra are scaled to similar heights for ease of comparison.  $g'$  values are indicated for several features; the six lines at  $g' = 2.07$  in the spectrum of  $\text{Mn}^{2+}$ SOD are most likely due to adventitious  $\text{Mn}^{2+}$  since MnSOD was never treated with EDTA.

Table 1: Metal Ion Content and Activity of SODs

sample	Fe content <sup>a</sup>	Mn content <sup>a</sup>	specific activity	% activity <sup>b</sup>
FeSOD	0.98	0	6700	100
apo-Fe-(Fe)SOD <sup>c</sup>	— <sup>d</sup>	—	<9	<0.1
Fe-rec-(Fe)SOD <sup>e</sup>	—	—	3882	58
Mn(Fe)SOD	0	0.50–0.95	8	0.1
MnSOD	0	0.98	6800	100

<sup>a</sup> On a per active site basis. <sup>b</sup> On a metal ion basis. <sup>c</sup> Not soluble enough to isolate and characterize (36). <sup>d</sup> Not measured. <sup>e</sup> Fe-reconstituted FeSOD, generated in small quantity by the same protocol as was used for Mn(Fe)SOD but under  $\text{N}_2$ .

signal at  $g = 2.0$  characteristic of  $\text{Mn}^{2+}$  bound in a symmetric environment, thus indicating that the  $\text{Mn}^{2+}$  is not bound extraneously. Since the Mn content is substoichiometric and the amount of Mn that could be bound correlated directly with the extent to which Fe was removed, it appears that the Mn binds in the active site. However, consistent with the seminal work of Yamakura (20, 38) Mn(Fe)SOD is completely inactive in the standard assay (Table 1). The somewhat variable substoichiometric binding of Mn lowers the spectroscopic signal intensities obtained but should not affect the nature of the signals observed or the activity of individual sites since MnSOD activity is directly proportional to the fraction of sites occupied by Mn (39).

Figure 2 compares the EPR spectrum of  $\text{Mn}^{2+}$ (Fe)SOD with that of  $\text{Mn}^{2+}$ SOD. Numerous turning points are visible in both spectra. The six-line  $\approx 90$  G splitting evident on several of these indicates that they derive from  $^{55}\text{Mn}^{2+}$ . The large number of features reflects the five possible  $\Delta m_S = \pm 1$  and  $\Delta m_I = 0$  EPR transitions, as well as formally forbidden  $\Delta m_S = \pm 1$  and  $\Delta m_I = \pm 1$  transitions mediated by zero-field interactions. Our spectrum of  $\text{Mn}^{2+}$ SOD is very much like previously published spectra (34), and the spectrum of  $\text{Mn}^{2+}$ (Fe)SOD is similar overall but differs in some of the exact positions of the features.

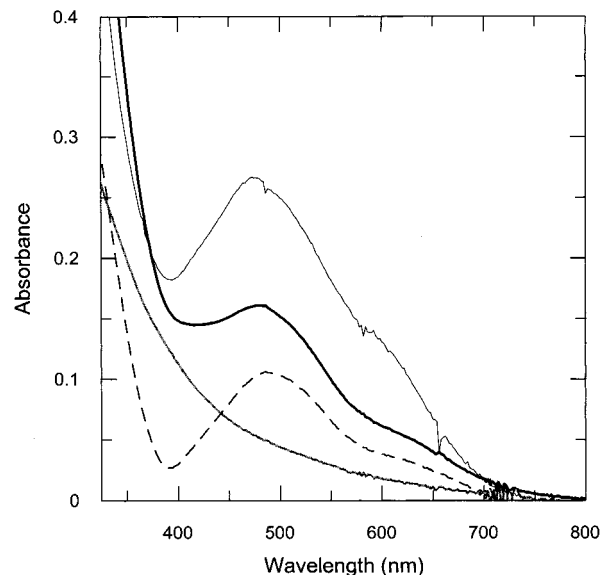


FIGURE 3: Optical spectra of  $\text{Mn}^{3+}$ SOD (top, thin line) and  $\text{Mn}^{3+}$ -(Fe)SOD (heavy black line).  $\text{Mn}^{3+}$ (Fe)SOD was generated upon oxidation of  $\text{Mn}^{2+}$ (Fe)SOD (gray line) with substoichiometric 100  $\mu\text{M}$   $\text{KMnO}_4$ . Subtraction of the spectrum of  $\text{Mn}^{2+}$ SOD from that of  $\text{Mn}^{3+}$ (Fe)SOD yields the difference spectrum plotted with the dashed line. 113  $\mu\text{M}$  Mn(Fe)SOD with 0.95 Mn per active site was used; thus an extinction coefficient for  $\text{Mn}^{3+}$  of 1000  $\text{M}^{-1} \text{cm}^{-1}$  at 486 nm is calculated from the  $\text{Mn}^{3+}$ (Fe)SOD –  $\text{Mn}^{2+}$ (Fe)SOD difference spectrum. The absorption maximum and shoulder of  $\text{Mn}^{3+}$ (Fe)SOD occur at 486 and 612 nm instead of at 478 and 600 nm as in  $\text{Mn}^{3+}$ SOD. Both SODs were suspended in 100 mM pH 7.8 potassium phosphate buffer.

Since the positions of the various turning points are indicative of the magnitude and symmetry of zero-field splitting, embodied by the parameters  $D$  and  $E$ , they reflect the geometry of the active site (40). Thus the signals at many similar  $g'$  values (e.g., between 700 and 3500 G) suggest that the active sites of  $\text{Mn}^{2+}$ (Fe)SOD and  $\text{Mn}^{2+}$ SOD are much alike. Nonetheless, the  $\text{Mn}^{2+}$ (Fe)SOD signal at  $\approx 300$  G, most likely representing a “zero-field” transition, indicates that  $D$  is smaller in  $\text{Mn}^{2+}$ (Fe)SOD than  $\text{Mn}^{2+}$ SOD (34), and the  $\text{Mn}^{2+}$ (Fe)SOD spectrum’s smaller distribution of  $g'$  values suggests that it is somewhat more rhombic and has a slightly larger  $E/D$  than  $\text{Mn}^{2+}$ SOD. Thus, the active site of  $\text{Mn}^{2+}$ (Fe)SOD is not exactly the same as that of  $\text{Mn}^{2+}$ SOD, but it is similar.

To compare the active sites in the oxidized state, the visible absorption and circular dichroism (CD) spectra of  $\text{Mn}^{3+}$ SOD and  $\text{Mn}^{3+}$ (Fe)SOD were obtained (Figure 3; CD courtesy of A. J. Lind, not shown). The signal from the oxidant  $\text{KMnO}_4$  could readily be distinguished from that of  $\text{Mn}^{3+}$ -(Fe)SOD on the basis of the former’s fine structure and is absent from the spectra shown because  $\text{KMnO}_4$  was added substoichiometrically and allowed to finish reacting with Mn-(Fe)SOD before the spectra were collected. The spectrum is clearly that of  $\text{Mn}^{3+}$ (Fe)SOD and not extraneous  $\text{Mn}^{3+}$  because the visible CD is similar in strength and features to that of  $\text{Mn}^{3+}$ SOD (A. J. Lind, A.-F. Miller, J. Xie, and T. Brunhold, unpublished). The long-wavelength band of  $\text{Mn}^{3+}$ -(Fe)SOD at 600 nm is shifted to 612 nm in  $\text{Mn}^{3+}$ (Fe)SOD, and the strongest absorbance is moved from 478 nm in  $\text{Mn}^{3+}$ -(Fe)SOD to 486 nm. These shifts in the  $\text{Mn}^{3+}$  d–d transitions are somewhat smaller than the more than 20 nm blue shift

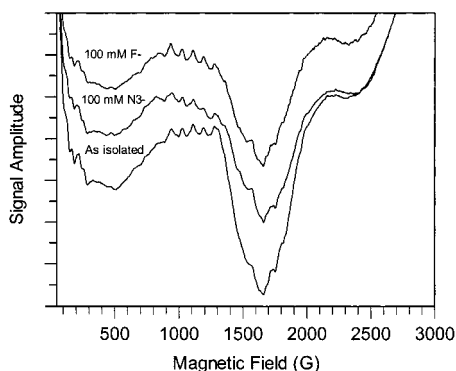


FIGURE 4: Substrate analogues do not appear to bind in the inner sphere of  $\text{Mn}^{2+}(\text{Fe})\text{SOD}$ .  $\text{Mn}^{2+}(\text{Fe})\text{SOD}$  in 100 mM pH 7.8 phosphate buffer was diluted with KF or  $\text{KN}_3$  solution to a final added anion concentration of 100 mM and then promptly frozen and observed by EPR as described in the Materials and Methods section.

of the ligand-to-metal charge transfer band responsible for the optical signal of  $\text{Fe}^{3+}(\text{Mn})\text{SOD}$ , relative to that of  $\text{Fe}^{3+}\text{-SOD}$  (30). The gross similarity of the visible spectra of  $\text{Mn}^{3+}(\text{Fe})\text{SOD}$  and  $\text{Mn}^{3+}\text{SOD}$  bespeaks similar active sites in the oxidized state as in the reduced state. Thus, we can interpret the chemistry of  $\text{Mn}(\text{Fe})\text{SOD}$  with reference to the active site of  $\text{MnSOD}$  in both oxidation states.

Figure 4 compares the EPR spectra of  $\text{Mn}^{2+}(\text{Fe})\text{SOD}$  as isolated with the spectra obtained upon addition of  $\text{N}_3^-$  or  $\text{F}^-$  to 100 mM. Although there is a slight change in the slope of the hump bearing the Mn hyperfine structure near 1000 G, the spectrum is basically unchanged. This suggests that  $\text{Mn}^{2+}(\text{Fe})\text{SOD}$  does not bind substrate analogues  $\text{N}_3^-$  and  $\text{F}^-$  in the inner sphere. The 100 mM  $\text{F}^-$  and  $\text{N}_3^-$  have been shown to significantly perturb the EPR signal of  $\text{Mn}^{2+}\text{SOD}$  (34) but not the magnetic CD (MCD) signal of  $\text{Fe}^{2+}\text{SOD}$  (41). Thus  $\text{Mn}^{2+}(\text{Fe})\text{SOD}$  resembles  $\text{Fe}^{2+}\text{SOD}$ , not  $\text{Mn}^{2+}\text{-SOD}$ , in not binding substrate analogues in the inner sphere. This does not mean it does not bind substrate and analogues, since  $\text{F}^-$  binds to  $\text{Fe}^{2+}\text{SOD}$ , just not in the inner sphere (42).

*Measurement of the  $E_m$  of MnSOD.* The apparent similarity of the environments of  $\text{Mn}^{2+}$  and  $\text{Mn}^{3+}$  in the two different

SOD proteins indicates that the inactivity of  $\text{Mn}(\text{Fe})\text{SOD}$  is not due to gross disruption of the active site. However, we have proposed that it can be explained by inappropriate redox tuning (31). To test this model for the case in which Mn is bound in each of the active ( $\text{MnSOD}$ ) and inactive [ $\text{Mn}(\text{Fe})\text{SOD}$ ] combinations, we have now compared the  $E_m$ s for the 2+/3+ couples of  $\text{MnSOD}$  and  $\text{Mn}(\text{Fe})\text{SOD}$ .

In contrast to the numerous published measurements of the  $E_m$  of  $\text{FeSOD}$  (16, 43), only a single attempt to determine that of  $\text{MnSOD}$  had yet been published at the time this work was done (44), and that was effectively unmediated. In addition, the oxidized state extinction coefficient required to interpret a titration was frequently not known, since many  $\text{MnSOD}$ s are isolated as a mixture of the oxidized and reduced states (34). Finally, SODs have proven to be extremely slow to equilibrate with mediators (31, 43). Therefore, to provide a good experimental value for comparison with computational studies (45) and the  $E_m$  of  $\text{Mn}(\text{Fe})\text{SOD}$ , we sought to improve upon the previous attempt to measure the  $E_m$  of  $\text{MnSOD}$ . Our criteria for validity are that the same  $E_m$  be obtained in ascending and descending titrations, that the titration be Nernstian, and that the  $E_m$  obtained be independent of the identity of the mediator used. While the current work was under review, titrations and the  $E_m$  of human  $\text{MnSOD}$  were reported (54).

Figure 5 shows a full redox titration of  $\text{MnSOD}$  in the presence of pBQ, based on the intensity of the  $\text{Mn}^{2+}\text{SOD}$  EPR signal near 1500 G (Figure 5, left side).  $\text{MnSOD}$  was reduced in steps by adding electrochemically generated  $\text{MV}^\bullet$  and then reoxidized in small steps by adding aliquots of  $\text{KMnO}_4$  before being rereduced again with  $\text{MV}^\bullet$ . The fraction reduced at each titration point was plotted vs potential and analyzed using the Nernst equation for reduction by a single electron, resulting in an  $E_m$  of  $290 \pm 15$  mV (Figure 5, right side). When the more general Nernst equation for reduction by  $n$  electrons is used, the  $E_m$  was not significantly different and  $n$  was 1.18, validating the  $E_m$  obtained but suggesting the possibility of some cooperativity in electron uptake by the two metal ions in the dimer. The potential obtained is significantly different from that of benzoquinone under the

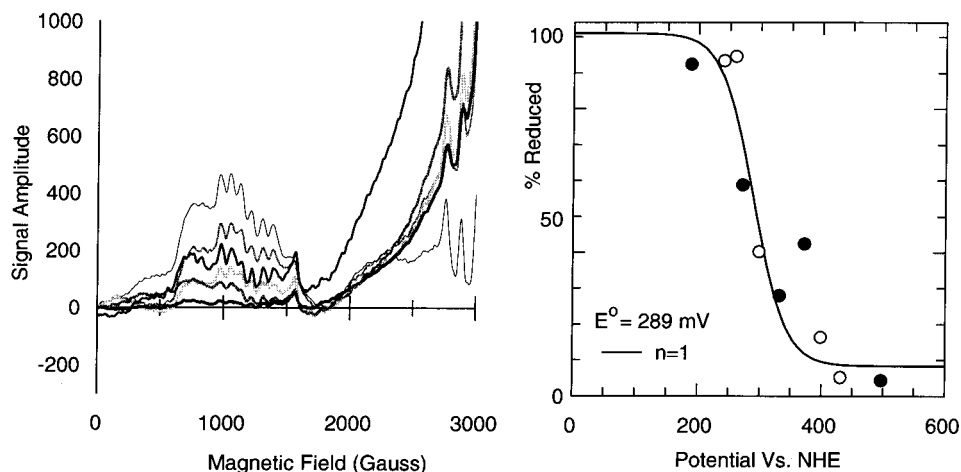


FIGURE 5: Potentiometric titration of  $\text{MnSOD}$  with pBQ as the mediator and using EPR to detect the concentration of  $\text{Mn}^{2+}\text{SOD}$  present. Left: The EPR signal of  $\text{Mn}^{2+}\text{SOD}$  near 1000 G is uncomplicated by the signals from pBQ $^\bullet$  and  $\text{MV}^\bullet$  at 3300 G. The spectra are baseline corrected using the WINEPR program provided by Bruker Instruments. Right: The fractional reduction  $\text{MnSOD}$  is plotted against the potential for both the oxidative (●) and reductive (○) titrations. All of the data are fit to the Nernst equation assuming a single electron event to yield an  $E_m$  of  $290 \pm 15$  mV. The solution conditions were as described in the Materials and Methods section. Note that SOD is extremely slow to equilibrate with mediators (31, 43, 49), and the titrations should properly be considered to be in quasi-equilibrium.

Table 2: MnSOD  $E_m$ s Obtained by Different Methods in mV vs NHE

mediator	DCIP	TMPD	pBQ	pBQ titration
mediator $E_m^a$	217	260	280	
MnSOD $E_m$	294 ± 15	296 ± 15	306 ± 15	263 ± 15

<sup>a</sup> Measured under the solution conditions used for equilibration with MnSOD.

same conditions (Table 2). The fact that the points obtained in the oxidative titration overlies those obtained in the reductive titrations indicates that the titration is fully reversible and that individual points reflect MnSOD at equilibrium with the potential read by the electrode. Adherence to the Nernst equation is adequate although there is some scatter in the data. This is largely due to errors in measuring EPR signal intensities and could contribute to the large value obtained for  $n$ . Finally, despite the duration of the titration and the presence throughout of pBQ, MnSOD retained 96% of its starting activity.

To ascertain that the  $E_m$  of MnSOD is independent of the mediator used, MnSOD was allowed to equilibrate with each of DCIP, pBQ, and TMPD, whose  $E_m$ s under our conditions are listed in Table 2. When reduced DCIP was used as a titrant *cum* mediator at a concentration 1/40th that of SOD dimers, the system equilibrated at 260 mV (after 30 h) and the  $E_m$  of MnSOD was calculated to be 290 ± 15 mV on the basis of the fractional oxidation of MnSOD. Similarly, equilibration with TMPD to 322 mV after more than 8 h yielded an  $E_m$  of 300 ± 15 mV. Thus,  $E_m$ s consistent with the  $E_m$  determined by titration were obtained with two different mediators, supporting an  $E_m$  for *E. coli* MnSOD of 290 mV. The difference between our value and that obtained for human MnSOD (54) may reflect interspecies differences.

*The  $E_m$  of Mn(Fe)SOD.* Whereas MnSOD is predominantly in the Mn<sup>3+</sup> state, Mn(Fe)SOD is isolated in the Mn<sup>2+</sup> state in air. Thus, it was immediately apparent that Mn(Fe)SOD's  $E_m$  is more positive than that of MnSOD (also see refs 31 and 37). Upper and lower limits were obtained for the  $E_m$  of Mn(Fe)SOD on the basis of the  $E_m$ s of the weakest oxidant able to oxidize Mn<sup>2+</sup>(Fe)SOD and the strongest oxidant unable to do so. We considered only oxidants able to oxidize Mn<sup>2+</sup>SOD and, therefore, most likely able to engage in electron transfer with Mn<sup>2+</sup>(Fe)SOD too. Of these, neither IrCl<sub>6</sub><sup>2-</sup> (897 mV) nor Mo(CN)<sub>8</sub><sup>3-</sup> (798 mV) could oxidize Mn<sup>2+</sup>(Fe)SOD, although Mn<sup>2+</sup>(Fe)SOD could be oxidized by stoichiometric MnO<sub>4</sub><sup>-</sup> [1230 mV (46)]. KMnO<sub>4</sub> oxidized Mn<sup>2+</sup>(Fe)SOD to which IrCl<sub>6</sub><sup>2-</sup> or Mo(CN)<sub>8</sub><sup>3-</sup> had already been added, indicating that neither of these interacts with Mn<sup>2+</sup>(Fe)SOD in such a way as to preclude its oxidation (Figure 6). Since even 10% oxidation by IrCl<sub>6</sub><sup>2-</sup> was not observed, the  $E_m$  of Mn(Fe)SOD is more than 60 mV above that of IrCl<sub>6</sub><sup>2-</sup> and falls between ≈960 and 1170 mV. Because these potentials are above that of water, it was not possible to obtain a full redox titration for Mn(Fe)SOD. Nonetheless, it is clear that its  $E_m$  is much higher than that of MnSOD and, moreover, higher than the potential for reduction of O<sub>2</sub><sup>•-</sup> to H<sub>2</sub>O<sub>2</sub> of 890 mV (47). This is sufficient to explain its inability to disproportionate O<sub>2</sub><sup>•-</sup>.

## DISCUSSION

A number of recent studies on metal-substituted SODs have implicated specific amino acid residues in their puzzling

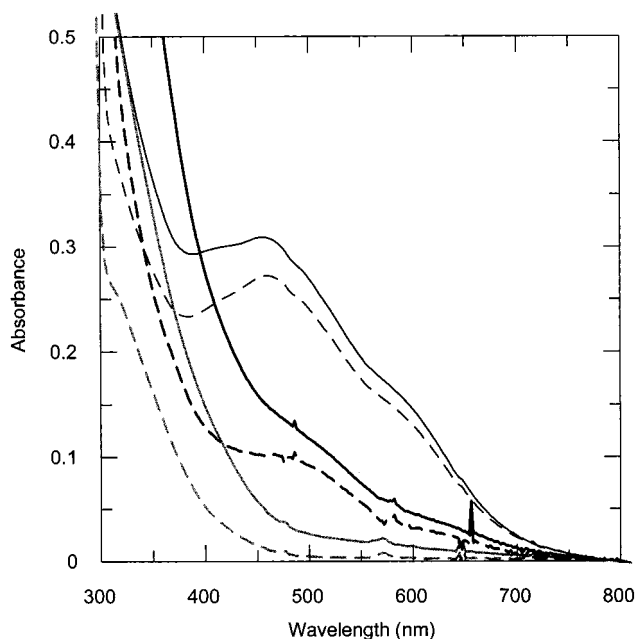


FIGURE 6: Mn(Fe)SOD is oxidized by KMnO<sub>4</sub> but not K<sub>2</sub>IrCl<sub>6</sub>. 100 μM Mn<sup>2+</sup>(Fe)SOD (gray dashed line) was degassed and treated with stoichiometric K<sub>2</sub>IrCl<sub>6</sub> with no effect on the spectrum other than the presence of the absorbance of IrCl<sub>6</sub><sup>2-</sup>, even after a day (gray solid line). However, upon subsequent addition of stoichiometric KMnO<sub>4</sub> to this sample, a hump appeared near 500 nm (heavy black line), which is best displayed upon subtraction of the Mn<sup>2+</sup>-SOD spectrum to yield the difference spectrum (heavy black dashed line). IrCl<sub>6</sub><sup>2-</sup> successfully and immediately oxidized partially reduced 150 μM MnSOD (thin black dashed line) to Mn<sup>3+</sup>SOD (thin solid black line). Both SODs were suspended in 100 mM pH 7.8 potassium phosphate buffer, as described in the Materials and Methods section.

inactivity (26–28, 48) and proposed thermodynamic bases for it (29, 31). However, most of these studies have focused on Fe(Mn)SOD. Therefore, we have now investigated the basis for the inactivity of Mn(Fe)SOD from *E. coli*. We have produced Mn(Fe)SOD following procedures similar to those used by Yamakura for *P. ovalis* FeSOD (20), although much harsher conditions were required to quantitatively extract active site Fe from *E. coli* FeSOD.

Comparison of the NMR, EPR, and optical spectra of *E. coli* FeSOD and Fe(Mn)SOD indicated that the metal ion geometry is similar in the two different proteins (30). Our current findings with Mn concur. Moreover, Fe bound to (Mn)SOD has a lower  $E_m$  than Fe bound to (Fe)SOD (31). We have now demonstrated that this too holds for Mn. Thus, for both Fe and Mn, the coordination geometry is similar in (Fe)SOD and (Mn)SOD, but the metal ion's potential is much lower in (Mn)SOD than in (Fe)SOD. This not only confirms our model for the basis for metal-substituted SODs' inactivity but also supports an underlying hypothesis that the redox tuning effect of the protein would be similar whether Mn or Fe were bound (31). Thus, the SOD system can be thought of as the sum of the effects of the metal ion and those of the protein, without a large cross term equivalent to cooperativity or coupling. This is consistent with the similar coordination geometries of the two sites since first-sphere differences would be more sensitive and responsive to the metal ion identity. Thus, redox tuning appears to stem from the outside the first coordination sphere.

Table 3:  $E_{m,s}$ s of 2+/3+ Couples of High-Spin Fe and Mn Compounds in mV vs NHE<sup>a</sup>

ligands	Fe complex	Mn complex	difference
(H <sub>2</sub> O) <sub>6</sub>	770	1510	740
EDTA	96	825	730
L, OH <sup>-b</sup>	-1230 <sup>c</sup>	-870 <sup>c</sup>	360
(Fe)SOD	220 <sup>d</sup>	>900	>680
(Mn)SOD	-240	290	530

<sup>a</sup> All  $E_{m,s}$  were measured in H<sub>2</sub>O except those of L-Fe-OH and L-Mn-OH, which were recorded in DMF. In DMF the  $E_{m,s}$  of the two superoxide dismutation half-reactions are -450 and 980 mV instead of -160 and 890 mV, respectively. <sup>b</sup> L=N[CH<sub>2</sub>CH<sub>2</sub>NC(O)NHC(CH<sub>3</sub>)<sub>3</sub>]<sub>3</sub>. <sup>c</sup> A. Borovik, personal communication. <sup>d</sup> Note that SOD is extremely slow to equilibrate with mediators (31, 43, 49), and the titrations should properly be considered to be in quasi-equilibrium. Thus, the SODs'  $E_{m,s}$  may incorporate substantial uncertainty despite our best efforts.

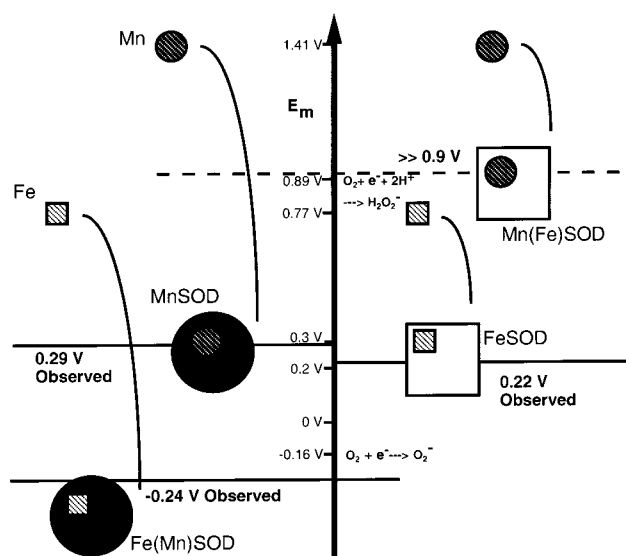


FIGURE 7: Reduction potentials of native and metal ion substituted SODs. Left to right: comparison of the different proteins. Top to bottom: different metal ions in same protein. Fe is denoted by small dark gray squares and (Fe)SOD by large light gray squares. Mn is depicted by small light gray circles and (Mn)SOD by large black circles. Note that SOD is extremely slow to equilibrate with mediators (31, 43, 49), and the titrations should properly be considered to be in quasi-equilibrium. Thus, the SODs'  $E_{m,s}$  may incorporate substantial uncertainty despite our best efforts.

The  $E_{m,s}$  of the 2+/3+ couples of both metal ions are lowered significantly in the SOD proteins relative to the hexaaquo complexes (Table 3), in part due to ligation by anionic Asp<sup>-</sup>. However, the difference between the  $E_{m,s}$  of Fe and Mn bound to a given SOD protein (either one) is comparable in magnitude to the difference between the  $E_{m,s}$  of Fe and Mn in homologous simple complexes (Table 3). This indicates that neither protein is somehow able to specifically tune the  $E_m$  of one metal ion more than that of the other but rather that each protein offsets both metal ions'  $E_{m,s}$  by approximately the same amount (Figure 7).

**Electronic Considerations.** The manifestation of the sum of the protein's and the metal ion's properties, and the result of the redox tuning, is the activity. In most systems one would naively expect that if a component required for activity were altered, another compensatory alteration would be necessary if the system were to retain activity. Alternately, if either one of two crucial components, here the protein or

the metal ion, were changed alone, one would expect that a change in activity would result.

In SODs, however, full activity can be obtained with a different metal ion in a protein that appears *not* to be substantially different. Yet Fe and Mn are quite different chemically, despite their relatively similar structural propensities. The electronic configuration of Fe in SOD catalysis is unlike Mn's in that Fe's 2+/3+ cycle corresponds to alternation between the d<sup>6</sup> and d<sup>5</sup> configurations but Mn cycles between d<sup>5</sup> and d<sup>4</sup>. The d<sup>5</sup> configuration occurs at the opposite point in the catalytic cycles and the d<sup>4</sup> configuration places a hole in d<sub>z<sup>2</sup></sub> whereas the d<sup>6</sup> configuration places an electron in one of the t<sub>2g</sub> orbitals, since both metal ions remain high spin in both proteins. Thus we conclude that the (Fe)SOD and (Mn)SOD proteins must in fact be significantly different from one another with respect to their effects on the reactivity of the bound metal ion.

The fact that high-spin Mn<sup>3+</sup> acquires the half-filled shell upon reduction whereas high-spin Fe<sup>3+</sup> loses it is an important contributor to Mn's much higher  $E_m$  in homologous simple high-spin complexes. Thus, if SOD proteins were to suppress the advantages of a half-filled shell, for example by providing strong ligand-field stabilization of either the d<sup>4</sup> or d<sup>6</sup> configuration, this would tend to depress the potential more for Mn or less for Fe, with the result that their  $E_{m,s}$  would be more similar when bound to a SOD protein than in simple model complexes that are less able to impose a strongly anisotropic environment [EDTA or (H<sub>2</sub>O)<sub>6</sub>, Table 3]. However, such a mechanism would not result in Fe's having an extra low  $E_m$  when bound to (Mn)SOD nor could it explain Mn's high  $E_m$  when bound to (Fe)SOD. The foregoing would be an example of an interactive effect.

Thus, our  $E_{m,s}$  argue against domination of redox tuning by strong ligand-field distortion of the metal ion electronic orbitals. The difference between the  $E_{m,s}$  of a given metal ion in the two different proteins is nonetheless very large indeed.

**The Significance of Proton Uptake Coupled to Reduction.** Whatever the source of the difference in redox tuning is, it is not readily apparent from the crystal structures.<sup>5</sup> We argue that it may be related to the protonation equilibria of the metal ion ligands, especially the coordinated solvent (26, 31). Since coordinated solvent is believed to take up a proton upon metal ion reduction (49), the coordinated solvent's pKs in both oxidation states necessarily contribute to the energy of the reduction *cum* protonation. A very low pK<sub>ox</sub> will tend to decrease the  $E_m$  whereas a low pK<sub>red</sub> will raise  $E_m$  much less since  $K_{red}$  is smaller than [H<sup>+</sup>] [eq 2, where  $K_{ox}$  and  $K_{red}$  are the acid dissociation constants of the oxidized and reduced states, respectively,  $E_{AH}$  is the reduction potential of the fully protonated species,  $E_m$  is the potential observed at a given pH, and pK = -log(K)].<sup>6</sup> In addition, protonation

$$E_m = E_{AH} + \frac{RT}{F} \ln \frac{K_{red} + [H^+]}{K_{ox} + [H^+]} \quad (2)$$

<sup>5</sup> The different active site conformation observed in the Fe(Mn)-SOD crystal structure can most simply be ascribed to the fact that this structure was obtained at a pH well above the pK ascribed to OH<sup>-</sup> binding (1) whereas the structure of MnSOD was determined at a pH well below the pK ascribed to OH<sup>-</sup> binding (53).

<sup>6</sup>  $E_{m,obs} = (RT/F) \ln([total\ reduced]/[total\ oxidized]) = (RT/F) \ln(((1 + K_{A,red}/[H^+])[AH^+_{red}])/(1 + K_{A,ox}/[H^+])[AH^+_{ox}]))$ .

of coordinated  $\text{OH}^-$  drastically changes its nature as a ligand from hard, charged with a strong ligand field to soft, neutral with a weak ligand field.

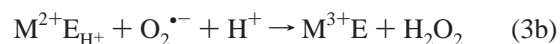
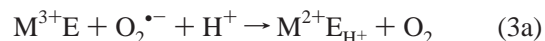
Coordinated solvent's  $pK_s$  could be modulated by the protein environment regardless of the metal ion identity and, thus, affect the  $E_m$ s of both metal ions similarly, to the extent that both are comparably sensitive to coordinated solvent's ionization state. Thus, if coordinated solvent's  $K_{ox}$  were raised more in (Mn)SOD than in (Fe)SOD, the  $E_m$ s observed in (Mn)SOD would be lower than those observed in (Fe)SOD. Modulation of a single  $pK$  is unlikely to account for the whole difference between the redox tuning of the two proteins as this would require that the  $pK_s$  in the two proteins differ by some 10 pH units. However, it could be an important factor.

*Differences in the H-Bonding between Coordinated Solvent and the Active Site Gln.* There is reason to believe that (Fe)-SOD and (Mn)SOD tune the  $pK_s$  of coordinated solvent differently. In both FeSOD and MnSOD coordinated solvent engages in two hydrogen bonds (H-bonds), which will modulate its  $pK_s$  (Figure 1). One H-bond is to the ligand  $\text{Asp}^-$  which also accepts an H-bond from the backbone. Since the distances between the heavy atoms involved are essentially identical in FeSOD and MnSOD, it seems unlikely that these could produce very different  $pK_s$  for coordinated solvent. However, the other group that H-bonds to coordinated solvent is the conserved Gln69/Gln146 of FeSOD/MnSOD,<sup>7</sup> which derives from different locations in the protein sequence and tertiary structure and represents the single most highly conserved difference between FeSODs and MnSODs [50, 51; see also the insightful discussion of Edwards et al. (52)]. In addition to its H-bond to coordinated solvent, this Gln H-bonds with the side chains of conserved Tyr34, Trp122, and Asn72 [numbering of FeSOD (17, 53)]. Thus it is itself subject to control by the rest of the SOD protein including residues in both domains.

Mutation of Gln146 of MnSOD dramatically affects activity (48, 52). Similarly, repositioning of the Gln of MnSOD to the position characteristic of FeSOD confers Fe-supported activity on MnSOD (26), and movement of the Gln characteristic of FeSOD to the position characteristic of MnSOD increases Mn-supported activity in *P. gingivalis* SOD (27). Finally, mutation of Gln146/Gln69 dramatically affects the  $E_m$  in both MnSOD (48) and FeSOD (Yikilmaz, Xie, Miller, and Brunold, unpublished).

Direct observation of the Gln side chain amide by <sup>15</sup>N NMR in  $\text{Fe}^{2+}$ SOD and  $\text{Fe}^{2+}$ (Mn)SOD indicates that it is much more strongly coupled to  $\text{Fe}^{2+}$  in Fe(Mn)SOD (26). This suggests significantly stronger H-bond donation to coordinated solvent in (Mn)SOD, which would tend to stabilize coordinated  $\text{OH}^-$  relative to coordinated  $\text{H}_2\text{O}$ , as observed in density functional calculations (Yikilmaz, Xie, Miller, and Brunold, unpublished). Since coordinated  $\text{OH}^-$  is associated with the oxidized state of SOD, the result would be greater depression of  $E_m$  by (Mn)SOD than (Fe)SOD, as observed here and in ref 31. Thus, stronger H-bond donation from Gln146 to coordinated solvent in (Mn)SOD (26) can provide a molecular mechanism capable of producing different  $pK_s$  for coordinated solvent in (Mn)SOD and (Fe)-SOD.

*Mechanistic Significance.* The protons of active site residues do not just tune the metal ion  $E_m$ ; at least two of them participate actively in the reaction. A proton is taken up upon reduction but is lost (to product) upon reoxidation of the metal ion. Thus:



where M signifies Mn or Fe, E signifies all non-metal ion components of the enzyme, and the  $\text{H}^+$  subscript indicates that the enzyme has acquired a proton. Although the same proton carriers need not be involved in individual steps of  $\text{H}^+$  uptake from solvent and transfer of  $\text{H}^+$  to nascent product, the coordinated solvent that is protonated in reaction 3a must be free to take up another proton at the end of reaction 3b, so it must release a proton.

As part of its effect on the  $E_m$ , depression of the  $pK_s$  of coordinated solvent in (Mn)SOD would make reaction 3a more difficult but favor reaction 3b, in effect countering the natural tendencies of Mn. However, this same effect would reinforce the natural tendencies of Fe and enhance Fe(Mn)-SOD's ability to conduct reaction 3b at the expense of reaction 3a by providing a proton for production of product. By contrast, (Fe)SOD could in effect raise the  $pK$  of coordinated solvent and have the reverse effect on the  $E_m$ s of both metal ions, complementing Fe's reducing tendency by disfavoring substrate reduction but reinforcing Mn's tendency to oxidize but not reduce  $\text{O}_2^{\bullet-}$  in Mn(Fe)SOD. Thus the same forces could be used in the two enzymes, in the opposite senses, so that in the native enzymes the protein's and metal ion's tendencies to oxidize or reduce are balanced; but if the metal ion and protein are mismatched, both components favor the same half-reaction with the result that the combination cannot complete the catalytic cycle (42). Indeed, Fe(Mn)SOD is active with respect to  $\text{O}_2^{\bullet-}$  reduction but inactive with respect to its oxidation (31).

Thus, while the mechanisms remain to be clarified, we have now shown that the different SODs of *E. coli* achieve the intriguing feat of applying very different  $E_m$  tuning similarly to two different metal ions but using essentially the same structural and ligand tools.

## CONCLUDING REMARKS

We have produced Mn(Fe)SOD devoid of Fe and with Mn specifically incorporated in the active site. Like Fe(Mn)-SOD, Mn(Fe)SOD is inactive under standard conditions. We report the  $E_m$  for *E. coli* MnSOD: 290 mV vs NHE. Furthermore, we demonstrate that the  $E_m$  of Mn(Fe)SOD is more than half a volt higher and greater than 960 mV. This independent test of our previous explanation for the inactivity of metal-exchanged SODs confirms our model (31). The apparently similar (Fe)SOD and (Mn)SOD proteins have dramatically different effects on the  $E_m$ s of their bound metal ions, and the effect is similar for both Fe and Mn and, thus, inherent to the protein. Since the active site Mn of Mn(Fe)-SOD appears not unlike that of MnSOD, in both oxidation states, based on EPR and optical spectroscopy, redox tuning appears to reside outside the first coordination sphere, as in (Fe)SOD (30). We propose that it stems from different H-bonding between coordinated solvent and the active site

<sup>7</sup> The residue numbering of *E. coli* SODs is used throughout.



Gln residue. The large magnitude of the differential redox tuning in *E. coli* FeSOD and MnSOD makes them an ideal system in which to develop the tremendous possibilities of redox tuning for enzyme redesign.

## ACKNOWLEDGMENT

We thank Amanda J. Lind for preliminary visible CD spectra and Prof. D. Barrick for use of the spectrometer.

## REFERENCES

- Edwards, R. A., Whittaker, M. M., Whittaker, J. W., Jameson, G. B., and Baker, E. N. (1998) *J. Am. Chem. Soc.* **120**, 9684–9685.
- Putnam, C. D., Arvai, A. S., Bourne, Y., and Tainer, J. A. (2000) *J. Mol. Biol.* **296**, 295–309.
- Ko, T. P., S. M., Musayev, F. N., Di Salvo, M. L., Wang, C. Q., Wu, S. H., and Abraham, D. J. (2000) *Acta Crystallogr., Sect. D* **56**, 241–245.
- Antonyuk, S. V., M.-A. V., Popov, A. N., Lamzin, V. S., Hempstead, P. D., Harrison, P. M., Artymyuk, P. J., and Barynin, V. V. (2000) *Crystallogr. Rep.* **45**, 105–116.
- Gatti, D. L., E. B., Ballou, D. P., and Ludwig, M. L. (1996) *Biochemistry* **35**, 567–578.
- Zhang, Z., Ren, J., Stammers, D. K., Baldwin, J. E., Harlos, K., and Schofield, C. J. (2000) *Nat. Struct. Biol.* **7**, 127–133.
- Rosenzweig, A. C., Frederick, C. A., Lippard, S. J., and Nordlund, P. (1993) *Nature* **366**, 537–543.
- Peters, J. W., Lanzilotta, W. N., Lemon, B. J., and Seefeldt, L. C. (1998) *Science* **282**, 1853–1858.
- Volbeda, A., Charon, M. H., Piras, C., Hatchikian, E. C., Frey, M., and Fontecilla-Camps, J. C. (1995) *Nature* **373**, 580–587.
- Joergers, R. D., Jacobson, M. R., Premakumar, R., Wolfinger, E. D., and Bishop, P. E. (1989) *J. Bacteriol.* **171**, 1075–1086.
- Butler, A. (1998) *Science* **281**, 207–210.
- Stintz, I. A., Barnes, C., Xu, L., and Raymond, K. N. (2000) *Proc. Natl. Acad. Sci. U.S.A.* **97**, 10691–10696.
- Oehlmann, W., and Auling, G. (1999) *Microbiology (Reading, U.K.)* **145**, 1595–1604.
- Boldt, Y. R., Sadowsky, M. J., Ellins, L. B. M., Que, J., L., and Wackett, L. P. (1995) *J. Bacteriol.* **177**, 1225–1232.
- Lavelle, F., McAdam, M. E., Fielden, E. M., Roberts, P. B., Puget, K., and Michelson, A. M. (1977) *Biochem. J.* **161**, 3–11.
- Barrette, W. C., Jr., Sawyer, D. T., Fee, J. A., and Asada, K. (1983) *Biochemistry* **22**, 624–627.
- Lah, M. S., Dixon, M. M., Patridge, K. A., Stallings, W. C., Fee, J. A., and Ludwig, M. L. (1995) *Biochemistry* **34**, 1646–1660.
- Stallings, W. C., Patridge, K. A., Strong, R. K., and Ludwig, M. L. (1984) *J. Biol. Chem.* **259**, 10695–10699.
- Ose, D. E., and Fridovich, I. (1976) *J. Biol. Chem.* **251**, 1217–1218.
- Yamakura, F. (1978) *J. Biochem.* **83**, 849–857.
- Martin, M. E., Byers, B. R., Olson, M. O. J., Salin, M. L., Aruneaux, J. E. L., and Tolbert, C. (1986) *J. Biol. Chem.* **261**, 9361–9367.
- Matsumoto, T., Terauchi, K., Isobe, T., Matsuoka, K., and Yamakura (1991) *Biochemistry* **30**, 3210–3216.
- Meier, B., Barra, D., Bossa, F., Calabrese, L., and Rotilio, G. (1982) *J. Biol. Chem.* **257**, 13977–13980.
- Yamakura, F., Kobayashi, K., Tagawa, S., Morita, A., Imai, T., Ohmori, D., and Matsumoto, T. (1995) *Biochem. Mol. Biol. Int.* **36**, 233–240.
- Yamakura, F., Rardin, R. L., Petsko, G. A., Ringe, D., Hiraoka, B. Y., Nakayama, K., Fujimura, T., Taka, H., and Murayama, K. (1998) *Eur. J. Biochem.* **253**, 49–56.
- Schwartz, A. L., Yikilmaz, E., Vance, C. K., Vathyam, S., Koder, R. L., Jr., and Miller, A.-F. (2000) *J. Inorg. Biochem.* **80**, 247–256.
- Hiraoka, B. Y., Yamakura, F., Sugio, S., and Nakayama, K. (2000) *Biochem. J.* **345**, 345–350.
- Whittaker, M. M., and Whittaker, J. W. (1997) *Biochemistry* **36**, 8923–8931.
- Yamakura, F., Kobayashi, K., Ue, H., and Konno, M. (1995) *Eur. J. Biochem.* **227**, 700–706.
- Vance, C. K., and Miller, A.-F. (1998) *Biochemistry* **37**, 5518–5527.
- Vance, C. K., and Miller, A.-F. (1998) *J. Am. Chem. Soc.* **120**, 461–467.
- Sorkin, D. L., and Miller, A.-F. (1997) *Biochemistry* **36**, 4916–4924.
- Slykhouse, T. O., and Fee, J. A. (1976) *J. Biol. Chem.* **251**, 5472–5477.
- Whittaker, J. W., and Whittaker, M. M. (1991) *J. Am. Chem. Soc.* **113**, 5528–5540.
- McCord, J. M., and Fridovich, I. (1969) *J. Biol. Chem.* **244**, 6049–6055.
- Beyer, J., W. F., Reynolds, J. A., and Fridovich, I. (1989) *Biochemistry* **28**, 4403–4409.
- Yamakura, F., Matsumoto, T., and Kobayashi, K. (1994) in *Frontiers of reactive oxygen species in biology and medicine* (Asada, K., and Yoshikawa, T., Eds.) pp 115–118, Elsevier Science, Amsterdam.
- Yamakura, F., and Suzuki, K. (1980) *J. Biochem. (Tokyo)* **88**, 191–196.
- Beyer, W. F., Jr., and Fridovich, I. (1991) *J. Biol. Chem.* **266**, 303–308.
- Whiting, A. K., Boldt, Y. R., Hendrich, M. P., Wackett, L. P., and Que, L., Jr. (1996) *Biochemistry* **35**, 160–170.
- Whittaker, J. W., and Solomon, E. I. (1988) *J. Am. Chem. Soc.* **110**, 5329–5339.
- Miller, A.-F. (2001) in *Handbook of metalloproteins* (Wiegand, K., et al., Eds.) Wiley and Sons, New York.
- Verhagen, M. F. J. M., Meussen, E. T. M., and Hagen, W. R. (1995) *Biochim. Biophys. Acta* **1244**, 99–103.
- Lawrence, G. D., and Sawyer, D. T. (1979) *Biochemistry* **18**, 3045–3050.
- Li, J., Fisher, C. L., Konecny, R., Bashford, D., and Noodleman, L. (1999) *Inorg. Chem.* **38**, 929–939.
- Shriver, D. F., and Atkins, P. W. (1990) in *Inorganic Chemistry*, W. H. Freeman and Co., New York.
- Sawyer, D. T. (1991) in *Oxygen Chemistry*, Oxford University Press, Oxford.
- Hsieh, H., Guan, Y., Tu, C., Bratt, P. J., Angerhofer, A., Lepock, J. R., Hickey, M. J., Tainer, J. A., Nick, H. S., and Silverman, D. N. (1998) *Biochemistry* **37**, 4731–4739.
- Bull, C., and Fee, J. A. (1985) *J. Am. Chem. Soc.* **107**, 3295–3304.
- Carlioz, A., Ludwig, M. L., Stallings, W. C., Fee, J. A., Steinman, H. M., and Touati, D. (1988) *J. Biol. Chem.* **263**, 1555–1562.
- Parker, M. W., Blake, C. C. F., Barra, D., Bossa, F., Schinina, M. E., Bannister, W. H., and Bannister, J. V. (1987) *Protein Eng.* **1**, 393–300.
- Edwards, R. A., Whittaker, M. M., Whittaker, J. W., Baker, E. N., and Jameson, G. B. (2001) *Biochemistry* **40**, 15–27.
- Edwards, R. A., Baker, H. M., Jameson, G. B., Whittaker, M. M., Whittaker, J. W., and Baker, E. N. (1998) *J. Biol. Inorg. Chem.* **3**, 161–171.
- Lévêque, V. J.-P., Vance, C. K., Nick, H. S., and Silverman, D. S. (2001) *Biochemistry* **40**, 10586–10591.